

Supporting Information

Anion Exchange Ionomers Enable Sustained Pure-Water Electrolysis using Platinum-group-metal-free Electrocatalysts

Yiwei Zheng¹, Ariana Serban¹, Haoyue Zhang², Nanjun Chen¹, Fang Song² and Xile Hu^{1*}

¹Laboratory of Inorganic Synthesis and Catalysis

Institute of Chemical Sciences and Engineering

Ecole Polytechnique Fédérale de Lausanne (EPFL)

Lausanne CH-1015, Switzerland

²State Key Lab of Metal Matrix Composites

School of Materials Science and Engineering

Shanghai Jiao Tong University (SJTU)

800 Dongchuan Rd., Minhang District, Shanghai 200240, China

*Corresponding author: Email: xile.hu@epfl.ch

Experimental

Anode Electrode Preparation

Two representatives of PGM and PGM-free OER catalysts (IrO_2 and NiFe-based catalysts) were used in this work. For PGM-free catalyst, both self-supported and powdery formats were synthesized. The method for self-supported PGM-free catalyst has been reported¹. Before deposition, nickel felt (2 cm x 2 cm, Dioxide Materials) was washed by HCl (10 wt%), DI water, ethanol, and acetone in sequence under sonication conditions for 10 min each, then dried at 60 °C. The catalyst on nickel felt was washed by DI water and denoted as self-supported NiFeOOH. This self-supported OER catalyst was directly used as anode electrode. The catalyst loadings were 20 mg/cm². The as-prepared self-supported NiFeOOH has not improved ECSA compared to its bare substrate (Figure S1a) as the growth of NiFeOOH has not largely changed the structure of Ni felt as shown in Figure S2b. The powdery NiFeOOH was typically prepared as follows: 1 M NaBH_4 was added dropwise to a solution containing 6.5 mM $\text{Ni}(\text{NO}_3)_2$ and 3.5 mM $\text{Fe}(\text{NO}_3)_3$, followed by vigorously stirring for 12 h. The precipitation was collected and washed with DI water and ethanol twice. The product was denoted as powder A. Powder B was synthesized by the same method, except for the use of the precursory solution of 10 mM $\text{Fe}(\text{NO}_3)_3$ only. Powder A and B were then mixed at a mass ratio of 5:1 by mechanical ball milling to obtain the powdery NiFeOOH.

Powdery NiFeOOH and IrO_2 (Alfa Aesar) were made into catalyst ink and then sprayed onto Ni felt porous transport layer (PTL). The method has been detailed in previous publications.^{2,3} The AEIs are NovaMea's branched poly(biphenyl piperidinium) ionomer (b-PBP)² with an ion exchange capacity (IEC) of 3.4 mmol/g (Figure 1 a) and Sustainion XB-7 (IEC = 2.2 mmol/g, Figure 1 b). The catalyst powder and DI water were added to the mortar and ground for 5 min. Next, an AEI was added at 15, 20, 25, and 30 % and PTFE powder was kept at 2 % of the mass

fraction in the catalyst layer. Then, the catalyst-AEI slurry was transferred to a centrifuge tube. Isopropyl alcohol (IPA) solvent was added until the IPA: DI water ratio was 9:1 by volume. The mixture was sonicated for 60 min. The water in the ultrasonic bath was maintained below 5 °C to avoid any AEI degradation and to avoid catalyst agglomeration. The ink dispersions were sprayed onto Ni felt PTL with an Iwata Eclipse HP-CS. For spraying, the carrier gas was 103 kPa (15 psig) ultra high purity (UHP) N₂. The catalyst loadings were kept at 3 mg/cm².

Cathode Electrode Preparation

Both PGM and PGM-free cathode electrodes were used. The preparation procedure of the PGM cathode is similar to the anode preparation for powdery OER catalyst, except that the AEI and PTFE powder contents were 20 % and 1.6 % of the total mass. The cathode PGM catalyst was Pt (weight fraction of 40 %) supported on Vulcan XC-72R (Alfa Aesar HiSPEC 4000). The ink dispersions were sprayed onto Toray TGP-H-060 PTLs with PTFE wetproofing (weight fraction of 5 %). The catalyst loadings were kept at 0.5 mg_{Pt}/cm².

A one-step potentiostatic electrodeposition procedure was used for manufacturing the self-supported PGM-free cathode on Toray TGP-H-060 PTL (C paper). The details of the procedure are described elsewhere.⁴ In brief, the catalyst is deposited by electrolysis at a negative current density in a deposition bath containing NiCl₂ and (NH₄)₆Mo₇O₂·4H₂O. The catalyst loadings were around 40 mg/cm². Ionomer-coated PGM-free cathode followed the procedure of spray coating with 1, 2, 5, and 10 wt% ionomer (b-PBP or Sustainion XB-7) of catalyst loading.

AEMWE Assembly and Break-in Procedure

25 μm NovaMea's branched poly(terphenyl piperidinium) AEM with 1 mol% of 1,3,5-triphenylbenzene comonomer (b-PTP-1, IEC = 2.81 mmol/g) was used in this study for performance test (Figure 1c).² Before cell assembly, the electrodes that contained ionomer and

AEMs were soaked in separate 1 M aqueous KOH solutions for 60 min, exchanging the solution twice during this time. After the 1 h soak, excess KOH was removed from the electrodes and AEMs and they were under extra DI water flush for pure water operation, then pressed together in the cell to form MEAs. The MEAs were loaded into 4 cm² Scribner hardware between single-pass serpentine flow nickel and graphite plates. The MEA was sealed and compressed with 10 mil (253 μm) and 6 mil (152 μm) PTFE for anode and cathode, respectively, at 2.5 N·m torque, resulting in 20 % - 25 % pinch. BiologicVMP-300 potentiostat with HCV-3048 booster was used to control operating current density. Cell temperature was controlled by a home-assembled temperature controller and sensor at 80 °C. The electrolyte flow rate was controlled by a peristaltic pump at 1 mL/min. The assembled water electrolyzers were flushed with pure water for 1 h then fed with pure water directly for activation process and measurement. The feed solution is DI water which has a pH ~ 7.

Before any data were taken, all cells underwent a break-in procedure. First, a cell was brought to its operating temperature while the liquid electrolyte is continuously fed into the anode side. Then the cell was operated galvanostatically, stepwise from 1 A to 4 A (1 A steps, held for a minimum of 30 min at each step), allowing the cell to equilibrate, and analyzing the cell's performance through linear sweep voltammetry, current hold, and electrochemical impedance spectroscopy (EIS) measurements. Galvano-EIS over a frequency range from 0.01 Hz to 100 kHz was performed by Autolab PGSTAT302N at 0.1 A/cm². EIS measurements were taken at the beginning and end of cell life, and when fresh electrolyte was refilled, to monitor the Ohmic changes. Multiple cells were constructed and tested for each measurement.

Anode and Cathode Potentials Measurement

Long AEM (Sustainion X37-50 grade T, 1.5 cm × 10 cm, thickness of 50 μm) was used in MEA and its extended part out of hardware worked as an ionic conductor to integrate an external reference electrode with Ag/AgCl reference electrode.⁵ The extended AEM entered a glass dish containing 1.0 M KOH electrolyte and was covered by 1.0 M KOH saturated Kimwipe to maintain hydration. Ag/AgCl reference potential was checked before and after measurement to ensure insignificant potential drift. The anode or cathode electrode potentials were then measured independently relative to the Ag/AgCl reference electrode. Importantly, the anode and cathode potentials measured with the reference electrode gave the same values as the full cell's potential in a two-electrode configuration. The thermodynamic potentials were calculated for OER and HER in 1.0 M KOH at 80 °C, to determine the overpotentials on the anode and cathode. Galvano-EIS was measured between the reference electrode and anode/cathode using the same setting as above to evaluate the Ohmic loss. The kinetics overpotentials for each electrode were determined by fitting a Tafel model to the Ohmic loss-free overpotential below 30 mA/cm². The mass transport overpotential was determined by subtracting the kinetics overpotential from the iR-free overpotential. (Equations below) Mass transport limitation in cathode refers to the water supply and bubble removal restrictions. As a thin membrane was used, water transport through membrane is immediate, therefore, the supply of water is sufficient though dry-cathode method is used; at the same time dry cathode ensures the production of dry H₂ which is beneficial in industrial applications. The active area of MEA was 1 cm². Multiple cells were constructed and tested for each measurement.

$$\eta_{\Omega} = iR_{\Omega}$$

$$E_{cell} - E_{rev} - \eta_{\Omega} = \eta_{kinetics} \propto a + b * \log i$$

$$\eta_{MT} = E_{cell} - E_{rev} - \eta_{\Omega} - \eta_{kinetics}$$

Electrochemical Test

Electrochemical tests were performed in 1 M KOH electrolyte (pH = 14). The working electrode was the as-prepared catalyst, and the Ag/AgCl and Pt wire were selected as the reference and counter electrode, repetitively. The potentials were calibrated to reversible hydrogen electrode (RHE) potentials. All the linear sweep voltammetry (LSV) was performed under 80% iR-compensation. The i and R were the tested current and the compensated resistance between the reference and the working electrodes, respectively. The equation: $\eta = E_{\text{RHE}} - 1.23 \text{ V}$, was used to calculate the overpotential (η). To weaken the capacitive current, all the LSV curves were tested under a sweep rate of 5 mV/s.⁶

Electrochemical active surface area (ECSA)

To understand the reaction mechanism of catalysts, the ECSA of the catalysts is investigated based on the electrochemical double-layer capacitance (C_{dl}). The C_{dl} can be calculated from cyclic voltammetry (CV) curves, which are tested in a certain potential window without the faradaic processes. In general, 6 consecutive CV curves at different sweep speeds (25 – 150 mV/s) are taken. The obtained CV curves are preferably close to the rectangle. After selecting the intermediate value of the applied potential range, the difference of current density under the current potential is calculated ($\Delta j = j_1 - j_2$), and the slope is obtained by linear fitting with different sweep speeds as X-axis and Δj as Y-axis. The slope is twice the value of C_{dl} . The larger value represents higher current density and more exposed surface reactive sites.⁷

Scanning Electron Microscopy (SEM)

Ultra-high resolution FE-SEM (Field Emission SEM Zeiss MERLIN scanning electron microscope) was used for SEM images and energy-dispersive X-ray spectroscopy (EDS) spectra. The electron beam energy in SEM and EDS was 5 and 20 k eV, respectively, using an

Everhart-Thornley secondary-electron (SE) detector. All images were taken with 150 X magnification.

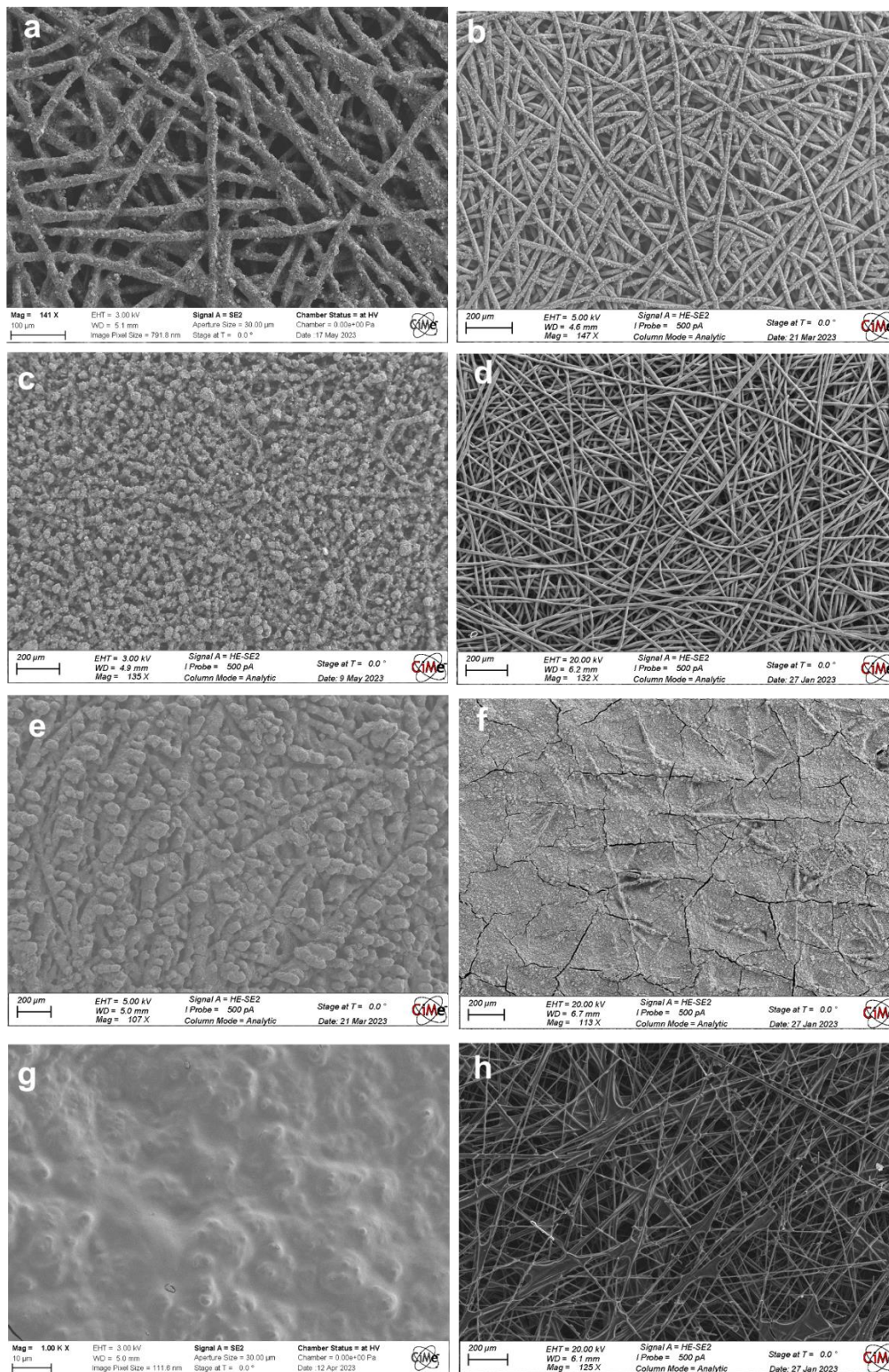


Figure S1. SEM images of OER catalysts: a) IrO₂-b-PBP-Ni felt, b) self-supported NiFeOOH-Ni felt, c) powdery NiFeOOH-b-PBP-Ni felt, d) bare Ni felt; HER catalysts: e) Pt/C-b-PBP-C paper, f) NiMo-C paper, g) NiMo-b-PBP-C paper and h) bare C paper.

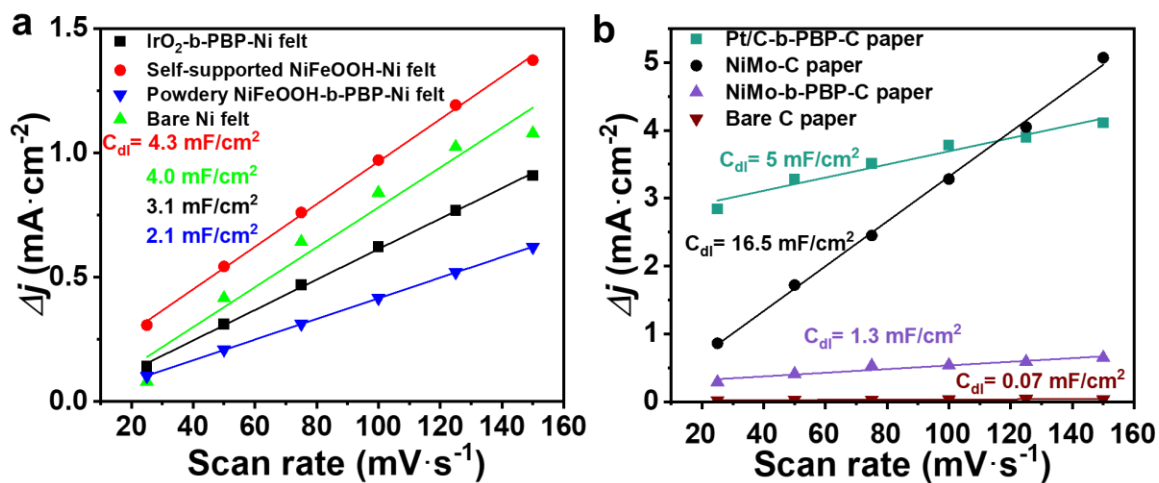


Figure S2. The C_{dl} values of catalysts (see Figure 2 of main text).

Table S1. ECSA values for catalysts.

	IrO₂-b-PBP-Ni felt	Self-supported NiFeOOH-Ni felt	Powdery NiFeOOH-b-PBP-Ni felt	Bare Ni felt	Pt/C-b-PBP- C paper	NiMo- C paper	NiMo-b-PBP-C paper	Bare C paper
ECSA (cm ²)	77.5	112	52.5	120	125	412.5	32.5	2.12

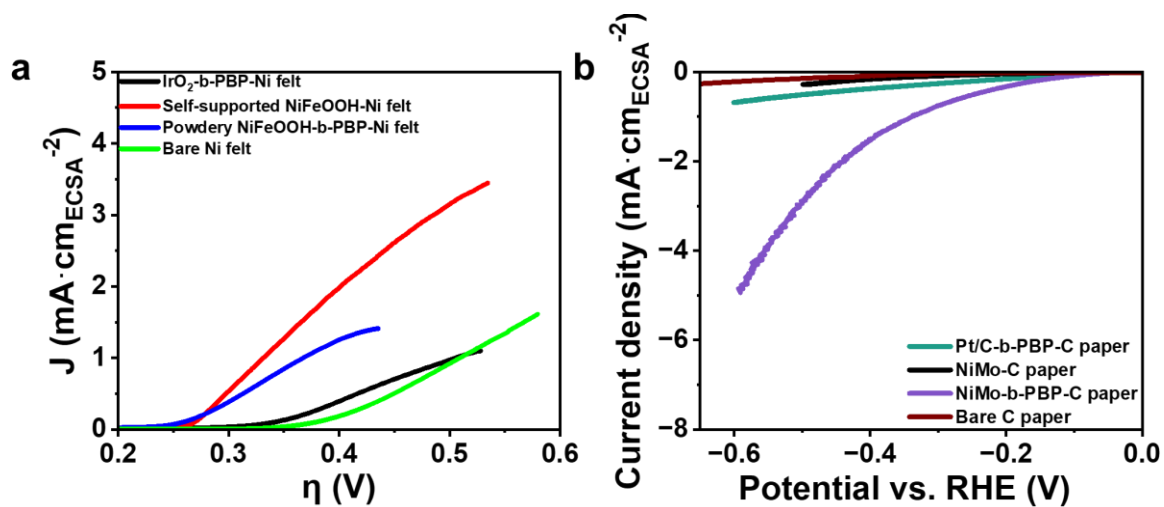


Figure S3. ECSA normalized LSV curves for a) OER b) HER catalysts from Figure 2.

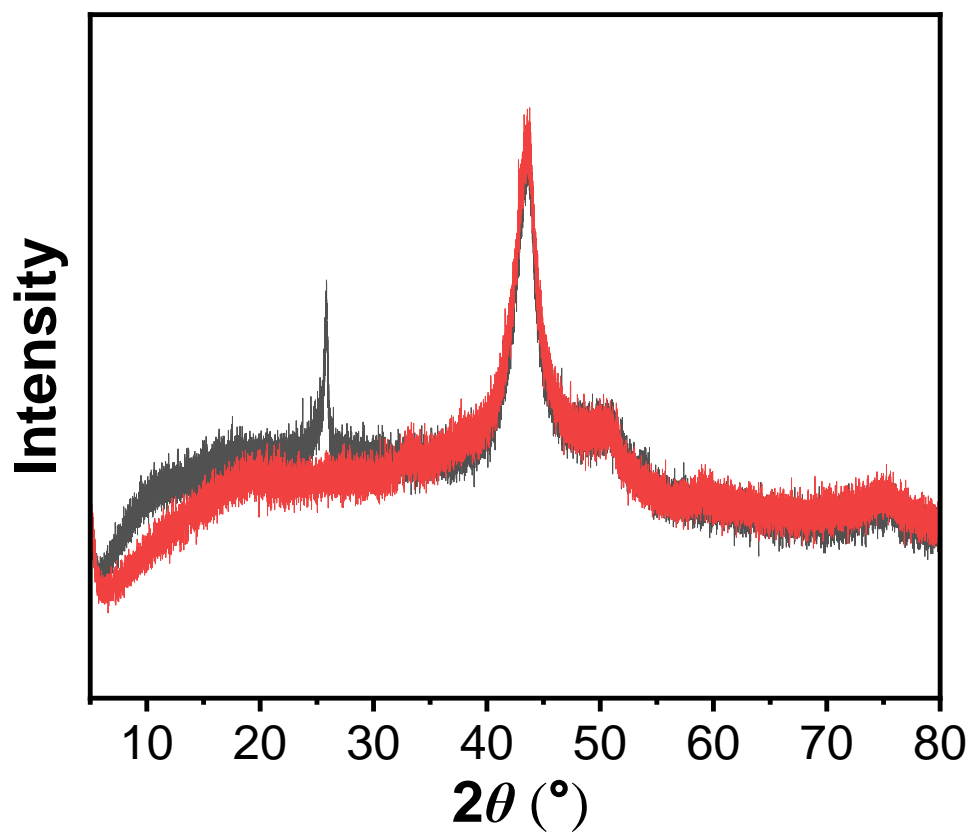


Figure S4. XRD of HER catalysts, red: NiMo-C paper, black: NiMo-b-PBP-C paper (peak $\sim 26^\circ$ belongs to impurities).

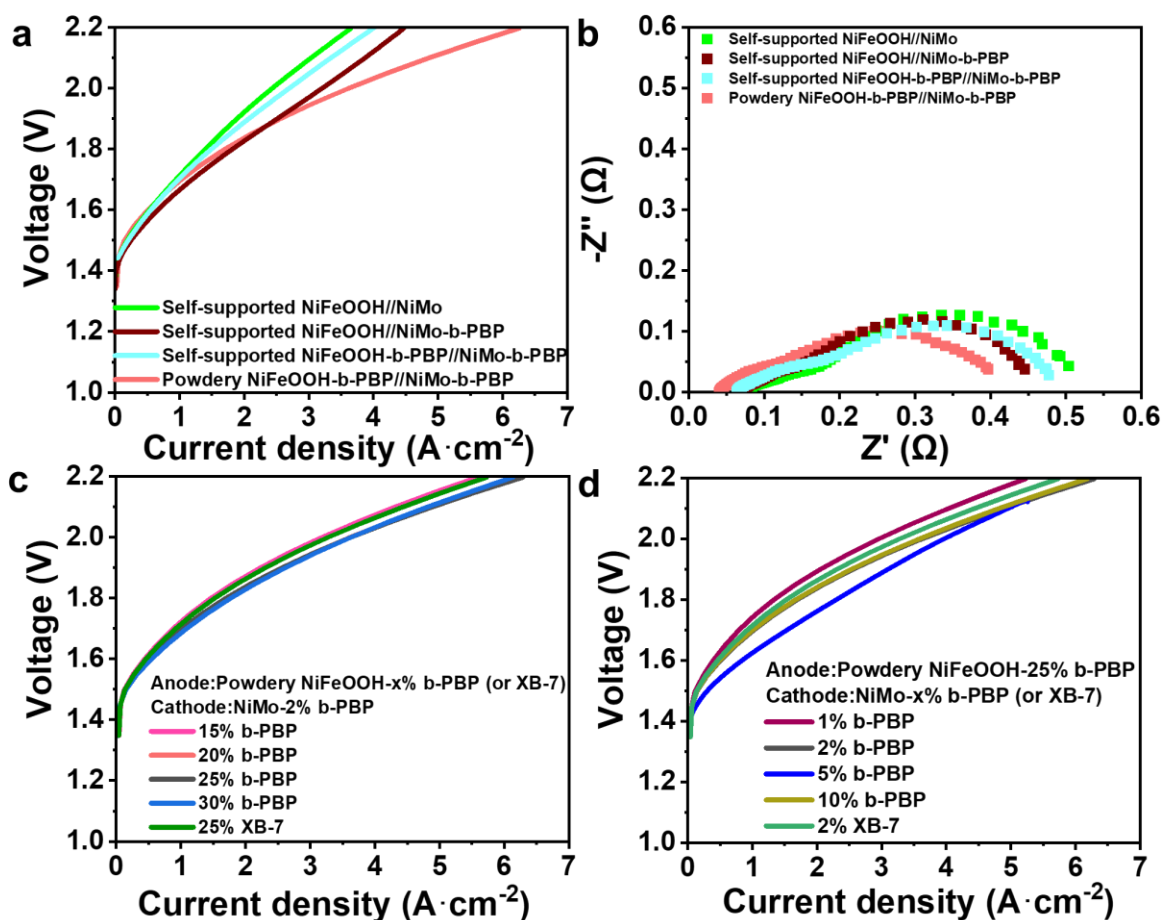


Figure S5. a) polarization curves of PGM-free AEMWEs showing the influences of ionomers operating in 1.0 M KOH, (anode ionomer: b-PBP, 20 wt%, cathode ionomer: b-PBP, 2 wt%); b) corresponding EIS measurements at 0.1 A/cm²; c) polarization curves of PGM-free AEMWEs w/ ionomer, anode ionomer contents vary from 15 wt% to 30 wt%, cathode ionomer was kept at 2 wt% (XB-7 with smaller IEC for 25 wt% case only); d) polarization curves of PGM-free AEMWEs w/ ionomer, anode ionomer was kept at 25 wt%, cathode ionomer was changing from 1 wt% to 10 wt% (XB-7 for 2 wt% case only). Cell and electrolyte temperatures at 80 °C.

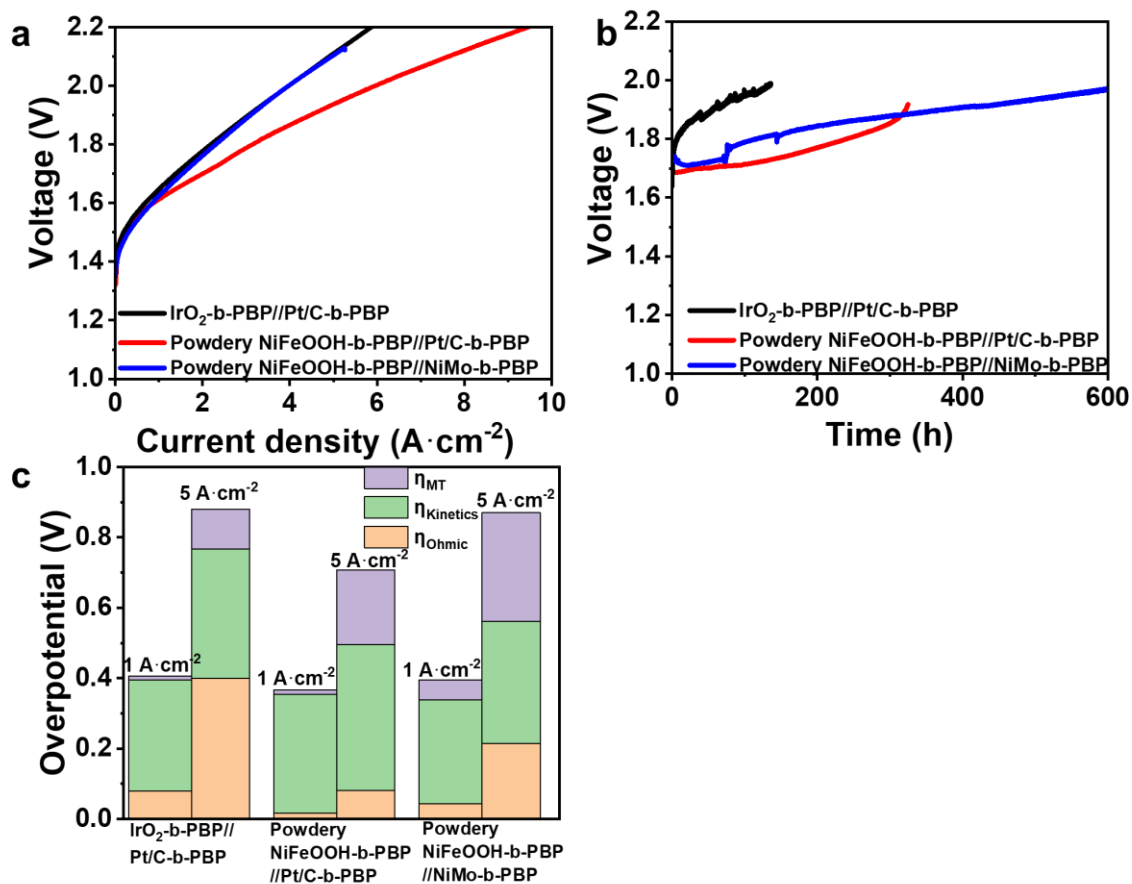


Figure S6. a) polarization curves of PGM//PGM, PGM-free//PGM, and PGM-free//PGM-free AEMWEs in 1.0 M KOH; b) stability at a constant current density of 1 A/cm²; c) performance loss distribution in 1.0 M KOH (at 1 and 5 A/cm²). Cell and electrolyte temperatures at 80 °C.

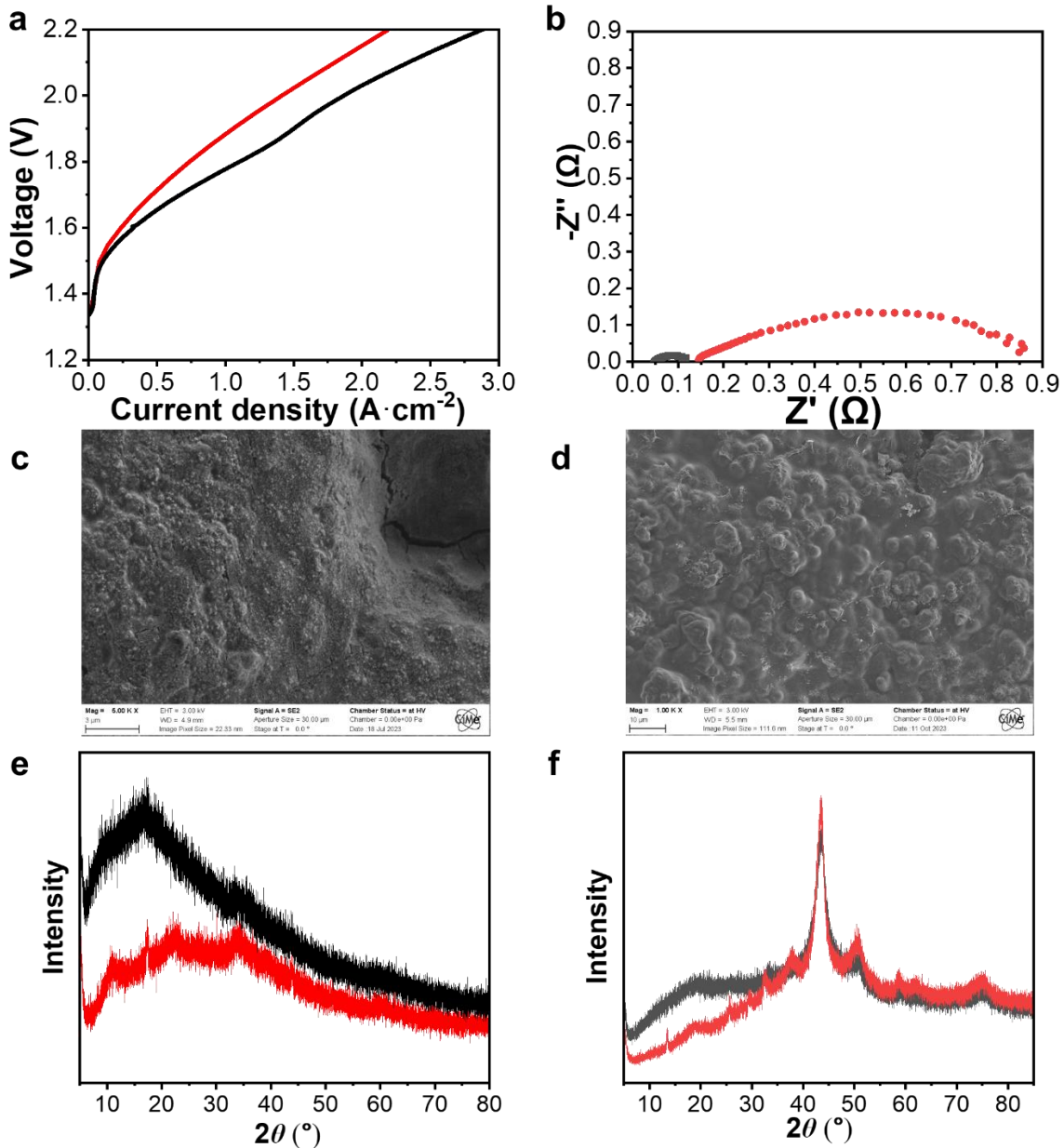


Figure S7. Post mortem MEA analysis from Figure 4 c. a) polarization curve in DI water (black: pristine, red: post mortem); b) corresponding EIS measurements at $0.1 A/cm^2$ (black: pristine, red: post mortem); SEM images of c) anode, d) cathode; XRD patterns of e) anode (black: pristine, red: post mortem), f) cathode (black: pristine, red: post mortem).

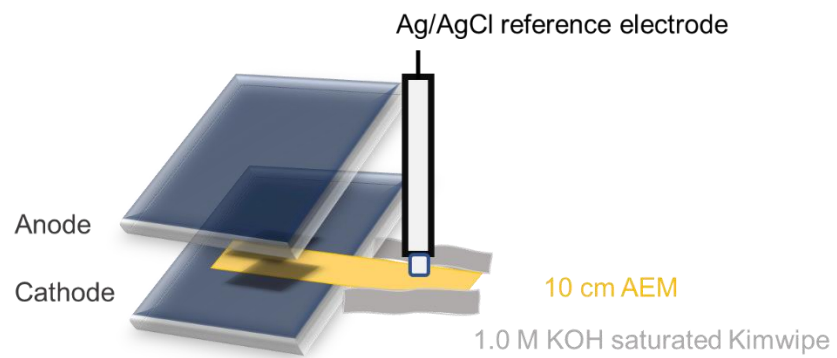


Figure S8. Scheme of three-electrode AEMWE with Ag/AgCl reference electrode.

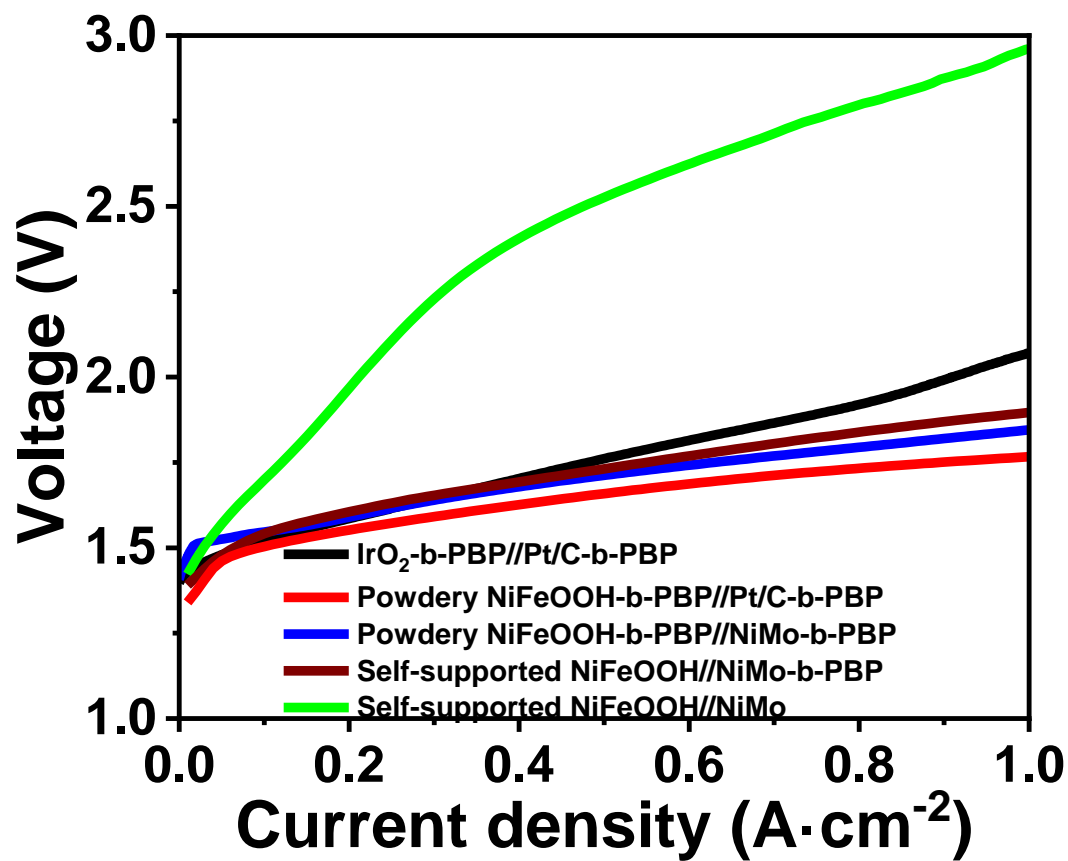


Figure S9. I-V curves in pure water of AEMWEs used for mechanistic studies of voltage losses. In this case a Sustainion X37-50 grade T AEM was used as it had the appropriate size.

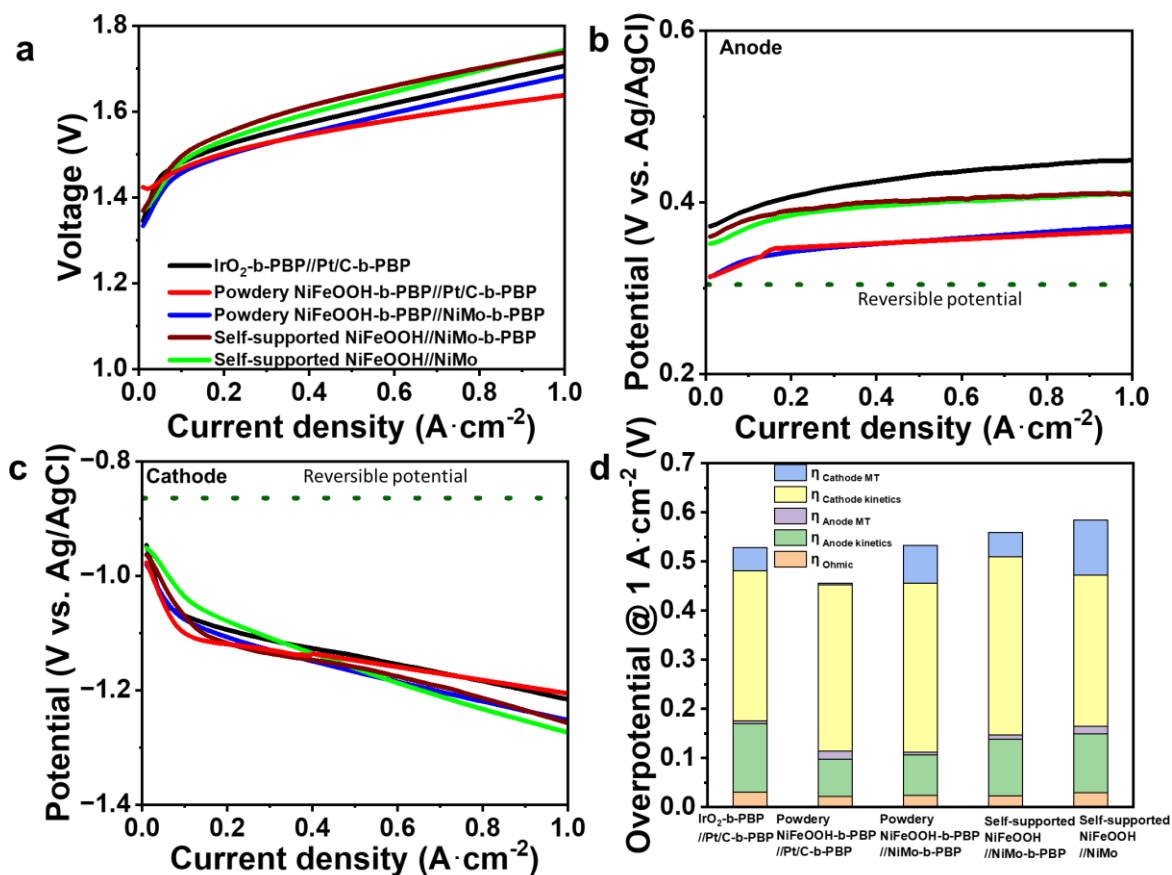


Figure S10. a), b) and c) for cell voltage, anode potential, and cathode potential of AEMWEs in 1.0 M KOH, respectively; d) overpotential breakdowns in 1.0 M KOH. Sustainion X37-50 grade T AEM.

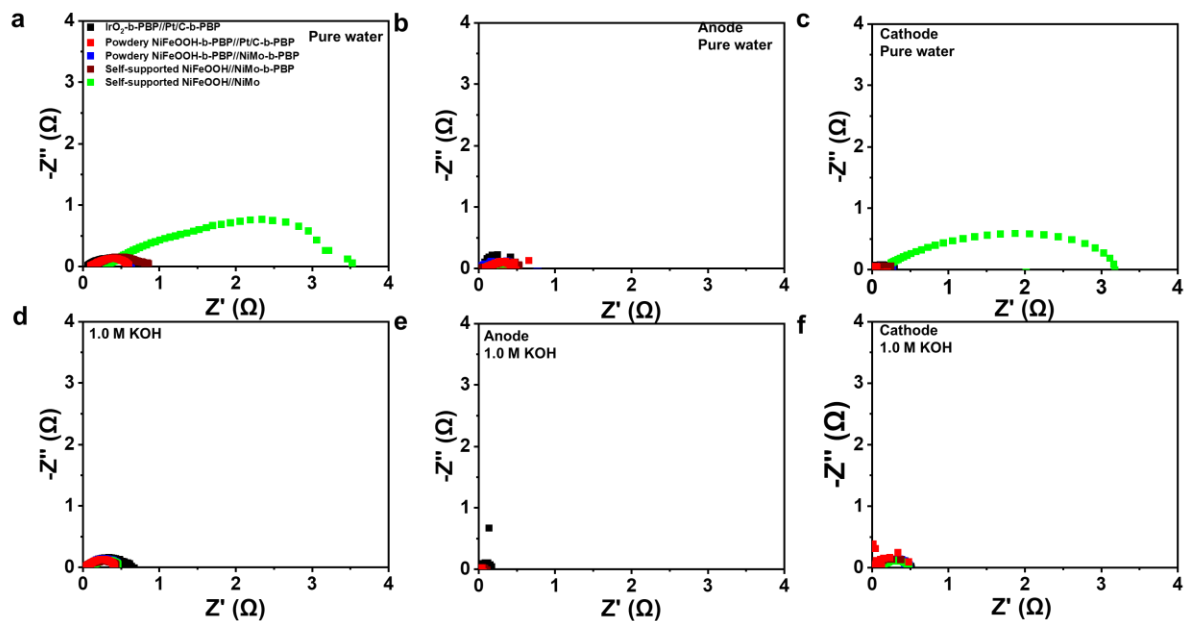


Figure S11. a) and d) EIS measurements for full cells in pure water and 1.0 M KOH, respectively; b) and e) EIS for anodes in pure water and 1.0 M KOH, respectively; c) and f) EIS for cathode in pure water and 1.0 M KOH, respectively. Cell and electrolyte temperatures at 80 °C. Membrane is Sustainion X37-50 grade T.

References

- (1) Zhang, Y.; Guo, P.; Niu, S.; Wu, J.; Wang, W.; Song, B.; Wang, X.; Jiang, Z.; Xu, P. Magnetic Field Enhanced Electrocatalytic Oxygen Evolution of NiFe-LDH/Co₃O₄ p-n Heterojunction Supported on Nickel Foam. *Small Methods* **2022**, *6* (6), 2200084. <https://doi.org/10.1002/smtd.202200084>.
- (2) Wu, X.; Chen, N.; Klok, H.-A.; Lee, Y. M.; Hu, X. Branched Poly(Aryl Piperidinium) Membranes for Anion-Exchange Membrane Fuel Cells. *Angewandte Chemie International Edition* **2022**, *61* (7), e202114892. <https://doi.org/10.1002/anie.202114892>.
- (3) Wu, X.; Chen, N.; Hu, C.; Klok, H.-A.; Lee, Y. M.; Hu, X. Fluorinated Poly(Aryl Piperidinium) Membranes for Anion Exchange Membrane Fuel Cells. *Advanced Materials* **2023**, 2210432. <https://doi.org/10.1002/adma.202210432>.
- (4) Serban, A.; Hu, X. Nickel Molybdenum Catalysts and Their Methods of Preparation.
- (5) Xu, Q.; Oener, S. Z.; Lindquist, G.; Jiang, H.; Li, C.; Boettcher, S. W. Integrated Reference Electrodes in Anion-Exchange-Membrane Electrolyzers: Impact of Stainless-Steel Gas-Diffusion Layers and Internal Mechanical Pressure. *ACS Energy Lett.* **2021**, *6* (2), 305–312. <https://doi.org/10.1021/acsenergylett.0c02338>.
- (6) Zheng, Y.; Jiao, Y.; Vasileff, A.; Qiao, S.-Z. The Hydrogen Evolution Reaction in Alkaline Solution: From Theory, Single Crystal Models, to Practical Electrocatalysts. *Angewandte Chemie International Edition* **2018**, *57* (26), 7568–7579. <https://doi.org/10.1002/anie.201710556>.
- (7) McCrory, C. C. L.; Jung, S.; Peters, J. C.; Jaramillo, T. F. Benchmarking Heterogeneous Electrocatalysts for the Oxygen Evolution Reaction. *J. Am. Chem. Soc.* **2013**, *135* (45), 16977–16987. <https://doi.org/10.1021/ja407115p>.